Structural Uncertainty Due to Fault Timing
A Multimodel Case Study from the Perth Basin

Bardot, Kerry; Lesueur, Martin; Siade, Adam J.; Lang, Simon C.; McCallum, James L.

DOI
10.1111/gwat.13429

Publication date
2024

Document Version
Final published version

Published in
Groundwater

Groundwater

Structural Uncertainty Due to Fault Timing: A Multimodel Case Study from the Perth Basin

by Kerry Bardot[1], Martin Lesueur[2,3], Adam J. Siade[2,4], Simon C. Lang[2], and James L. McCallum[2]

Abstract

Faults can fundamentally change a groundwater flow regime and represent a major source of uncertainty in groundwater studies. Much research has been devoted to uncertainty around their location and their barrier-conduit behavior. However, fault timing is one aspect of fault uncertainty that appears to be somewhat overlooked. Many faulted models feature consistent layer offsets, thereby presuming that block faulting has occurred recently and almost instantaneously. Additionally, barrier and/or conduit behavior is often shown to extend vertically through all layers when a fault may in fact terminate well below-ground surface. In this study, we create three plausible geological interpretations for a transect in the Perth Basin. Adjacent boreholes show stratigraphic offsets and thickening which indicate faulting; however, fault timing is unknown. Flow modeling demonstrates that the model with the most recent faulting shows profoundly different flow patterns due to aquifer juxtaposition. Additionally, multiple realizations with stochastically generated parameter sets for layer, fault core, and fault damage zone conductivity show that fault timing influences flow more than layer or fault zone conductivity. Finally, fault conduit behavior that penetrates aquitards has significant implications for transport, while fault barrier behavior has surprisingly little. This research advocates for adequate data collection where faults may cause breaches in aquitards due to layer offsets or conduit behavior in the damage zone. It also promotes the use of multiple geological models to address structural uncertainty, and highlights some of the hurdles in doing so such as computational expense and the availability of seamless geological-flow modeling workflows.

Introduction

Sedimentary basins are typically comprised of laterally extensive geological layers which create predictable flow regimes. However, layer discontinuity caused by structural elements such as faults, pinch outs, unconformities, and paleo-incisions can dramatically transform a groundwater flow field. Therefore, uncertainty around the presence and nature of these structural elements can undermine the reliability of groundwater model predictions (Bredehoeft 2005; Zhou and Li 2011), even more so than hydraulic parameter uncertainty (Hojberg and Refsgaard 2005; Seifert et al. 2012). Often an incorrect structural model is compensated by parameter bias, resulting in good history matching, but often leading to biased predictions (Bredehoeft 2005).

However, despite its well-known significance, structural uncertainty analysis is often excluded from groundwater modeling workflows (Refsgaard et al. 2006) for a number of reasons. Firstly, a multimodel approach is recommended when addressing structural uncertainty (Enemark et al. 2019), but incorporating multiple geological models in the modeling process is undoubtedly challenging. Geological modeling is typically cumbersome and labor-intensive with limited options for free, yet sophisticated geological modeling software capable of generating multiple structural models. Even commercial software that can generate the realizations of geological models uses stochastic grid population of lithology type (e.g., LeapFrog, GoCAD) and is unable to generate multiple interpretations of structural concepts such as faults and unconformities (Grose et al. 2021). Secondly, there appears to be a lack of seamless interfacing between geological and flow modeling software, which restricts inverse modeling of structural concepts because structural

[1]Corresponding author: School of Earth Sciences, University of Western Australia, Perth, Australia; kerry.bardot@research.uwa.edu.au

[2]School of Earth Sciences, University of Western Australia, Perth, Australia; martin.lesueur@uwa.edu.au; adam.siade@csiro.au; simon.lang@uwa.edu.au; james.mccallum@uwa.edu.au

[3]Civil Engineering and Geosciences, Delft University of Technology, Netherlands; martin.lesueur@uwa.edu.au

[4]CSIRO Environment, Wembley, WA, Australia; adam.siade@csiro.au

Article impact statement: Stratigraphy in the vicinity of faults is typically not considered and can greatly impact groundwater flow.

Received January 2024, accepted June 2024.

doi: 10.1111/gwat.13429

parameters cannot be manipulated autonomously based on feedback from flow model results (Pham and Tsai 2016). Another complicating issue is that of spatial discretization. While inverse modeling of parameters relies on repeated modification of cell properties (White et al. 2020), inverse modeling of structural concepts becomes more complicated given that spatial discretization should be based on geological structure (Bardot et al. 2022). Changing structural scenarios, and hence discretization, when using a multimodel approach becomes logistically challenging. Fortunately, progress is being made toward incorporating structural uncertainty into the modeling process including flexible discretization techniques (Langevin et al. 2017; HydroAlgorithmics 2020), parameterization of structural concepts (Marshall et al. 2019), and model averaging techniques (Li and Tsai 2009; Refsgaard et al. 2012). Studies that have employed a multimodel approach to deal with structural uncertainty have typically considered layering combinations in shallow sedimentary systems (Troldborg et al. 2007; Rojas et al. 2008; Seifert et al. 2012), as well as the distribution of channels (Michael et al. 2010; Rongier et al. 2017). Fewer studies have focused on uncertainty around faults (Ainsworth 2006; Marshall et al. 2019).

Faults can profoundly impact groundwater flow in two ways. Firstly, deformation processes modify rock permeability within the fault zone causing either barrier, conduit, or combined barrier-conduit hydraulic conditions (Caine et al. 1996; Bense et al. 2013). Secondly, faulting typically offsets geological layers causing flow along an aquifer to be restricted or even sealed if juxtaposed against an aquitard, or for substantial throw, for two different aquifers to be hydraulically connected (Allan 1989; Knipe 1997; Yielding et al. 1997). Much research has been undertaken on fault zone permeability conceptualization and its effect on fluid flow (Bense and Person 2006; Manzocchi et al. 2010; Ortiz et al. 2019; Poulet et al. 2021), and indeed models of faulted aquifers often consider the barrier-conduit nature of faults (Leray et al. 2012; Marshall et al. 2019; Hadley et al. 2020). While the importance of fault block juxtaposition and flow compartmentalization has been asserted and showcased (Bense and Person 2006; Nishikawa et al. 2009; McCallum et al. 2021), faulted aquifer studies tend to overlook the significance of fault timing and the subsequent arrangement of sedimentary layers adjacent to the fault (Hadley et al. 2020; Sproule et al. 2021; Casillas-Trasvina et al. 2022).

Stratigraphy along faults is complex and results from a complicated interplay between rock type, tectonics, and deposition over hundreds of millions of years. The result is an assortment of fault styles and deformation of facies adjacent to faults (Schlische and Anders 1996). Most often, fluid flow models assume that faulting occurs at the end of a sedimentary sequence, resulting in a *block fault* with uniform thickness and offset of layers (Manzocchi et al. 1999; Bense and Person 2006; Manzocchi et al. 2010; McCallum et al. 2021). However, faulting often occurs concurrently during deposition, resulting in *growth faults* where sedimentary sequences become thicker and warped adjacent to the fault on the footwall side. Understanding fault type and timing is critical for predicting groundwater flow, as the offset of aquitards may result in hydraulic connection of otherwise vertically isolated aquifers (Allan 1989). In addition to this, fault timing affects the vertical extent of the fault zone which could significantly influence near surface hydrogeology if faults are recent and propagate to near surface. On the contrary, older faults may be of little importance if hydrogeological units are not significantly offset and if the fault is covered by an unconformity.

Unfortunately, the characterization of faults and sequence geometry predominantly relies on seismic imaging techniques, which are costly and prohibitive in built-up areas, leaving hydrogeologists to rely on sparse lithological logs and arbitrary interpolation to create geological models. Although downhole geophysics and palynology assist in understanding ancient depositional environments, and therefore sedimentary architecture (Ainsworth 2005; Scharling et al. 2009), there always remains uncertainty in fault architecture without adequate seismic data.

To our knowledge, there are no hydrogeological studies that consider uncertainty around fault timing and the implication for flow modeling. Using a study site, we identify multiple plausible scenarios of fault timing and develop matching structural interpretations of stratigraphy in proximity to the faults. We then examine the effect of the different structural models on long-term groundwater flow predictions, and by doing so, evaluate the importance of fault timing in groundwater models. We also compare the relative importance of aquifer juxtaposition with fault permeability effects at a regional scale.

Study Area

A study area within the Perth Basin (Figure 1) was selected to investigate the effect of fault timing on groundwater flow for several reasons. Firstly, the sedimentary basin has experienced many tectonic stages over a large time scale (Permian to Cretaceous) resulting in faults that have occurred at different points in time. Secondly, the area is within the metropolitan area where traditional seismic imaging is not straightforward to obtain, resulting in much uncertainty around fault geometry, and therefore fault timing. Furthermore, the area presents environmental and economic significance given that water supply abstraction and re-injection of treated wastewater are occurring in proximity to the fault.

The Perth Basin is an elongated north–south rift basin extending 1300 km along the south-west coast of Australia, bound by the Darling Fault on its eastern edge (Figure 1). The basin was formed from extended rifting and breakup of the continental margin during the early Cretaceous (Mory and Iasky 1996) and has a complex multistage history resulting in a combination of structural elements. The basin is compartmentalized at multiple scales by N-NNW striking normal faults,

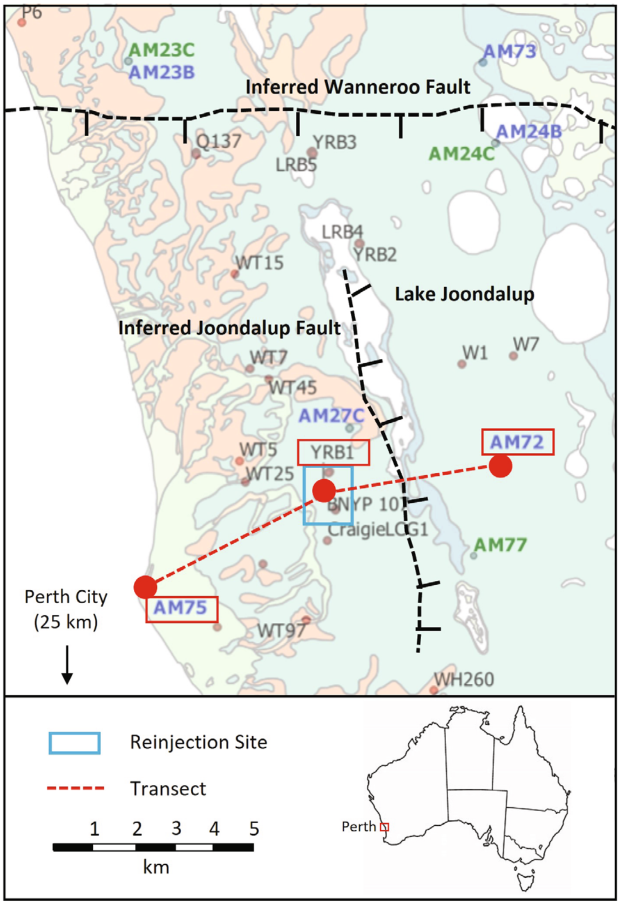

Figure 1. Study area within the Perth Basin showing potential presence of faults (dashed black lines), and the transect used in this study (dashed red line). Monitoring bores shown in green are installed into the Leederville Aquifer and blue into the Yarragadee Aquifer. Black labels represent pumping bores in either the Leederville or Yarragadee aquifers. The main surface feature is the elongated Lake Joondalup.

both planar and listric, as well as dextral strike-slip (Song and Cawood 2000). Significant rifting and breakup in the late Jurassic and early Cretaceous have caused major structural features in the basin, predominately north striking normal faults dividing the basin into troughs and ridges, which are bound by west–east transfer faults (Song and Cawood 1999; Olierook et al. 2015).

Sedimentary sequences extend to a depth of up to 12 km (Davidson 1995), with depositional environments varying dramatically over time. Sequences pertaining to this study are from the late Jurassic to early Cretaceous, as presented in Figure 2. This study focuses on faulting during the deposition of the Warnbro Group, which overlies the Neocomian Unconformity and eroded by the Aptian Unconformity (Davidson 1995). These units range from marine to marginal marine to fluvial environments due to multiple flooding events. Major hydrogeological units from oldest to youngest include the Yarragadee Aquifer (typically >2000 m thick), South Perth Shale Aquitard (50 to 230 m), Leederville Aquifer (200 to 300 m), Coolyena Group Aquitard (0 to 20 m), and the overlying Superficial Aquifer (typically 20 to 30 m saturated thickness) (Davidson 1995).

Although faults are likely to be present at multiple scales beneath metropolitan Perth, few have been confirmed (Thomas 2014). Unlike offshore areas where structural analysis has been undertaken for hydrocarbon resource development (Crostella and Backhouse 2000), relatively little has been done for the onshore component of the basin. Physical access and financial resource limitations for investigations in built-up areas have led to a limited understanding of faulting within Perth's major groundwater supplies. Perth's Regional Aquifer Modelling System (PRAMS) (De Silva et al. 2013) currently incorporates some known and inferred faults conceptually as hydraulic flow barriers (HFBs). The geological model that serves the basis for the flow model is updated periodically by incorporating the most recent drilling data and interpretation.

A transect crossing a suspected fault in the northern Perth Basin, from herein the "Joondalup Fault," was selected to study the impact of stratigraphy interpretation on groundwater flow (Figure 1). The existence of the Joondalup Fault is unconfirmed and based only on sparse stratigraphic records which indicate offsets and thickening of some units, in particular the South Perth Shale, toward the fault. Without seismic data, the exact location and structure of the fault is also unknown. Hydrogeological data are also too sparse to either confirm or disprove the presence of the fault. Therefore, in the absence of seismic data, which is often the case for groundwater studies, stratigraphy interpolation becomes a subjective task with multiple feasible interpretations.

Model Setup

Geological Models

A transect across the inferred fault was developed using three deep bores, AM75, YRB1, and AM72, all installed into the Yarragadee Aquifer (Figure 3). Lithology was depicted using visual logging during drilling, palynology, and gamma logs. Individual minor stratigraphic sequences were not easily identified across the three logs given the large distance between the bores and extensive presence of tidal and alluvial paleo-channels in the Wanneroo Member; however, major sequence correlations are shown in Figure 3. The logs indicate that a fault is highly probable between YRB1 and AM72 due to both offsets in stratigraphy (bottom of South Perth Shale in YRB1 354 m higher than AM72 4.3 km away) and thickening of strata (52 m in YRB1 compared to 230 m in AM72). However, offsets and thicknesses between all Warnbro Group units are not consistent, indicating a complex regime of deposition and tectonics, and therefore increased uncertainty about aquifer connectivity across the fault.

Therefore, in the absence of seismic data and because of the remaining uncertainty around the structural configuration between YRBB1 and AM72, a multimodel approach was adopted. Three plausible structural models

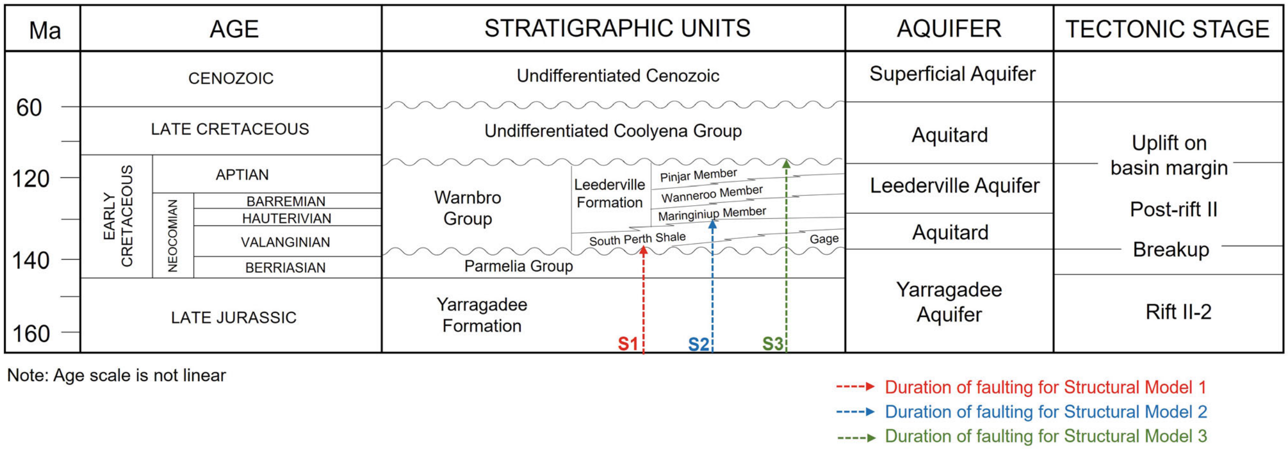

Figure 2. Simplified stratigraphic column for the northern Perth Basin which focuses on units deposited during the Early Cretaceous where suspected faulting of the Leederville Aquifer has occurred. Major aquifers and tectonic stages are shown (modified from Leyland 2012; Olierook et al. 2015), as well as the duration of faulting assumed for each structural models S1, S2, and S3.

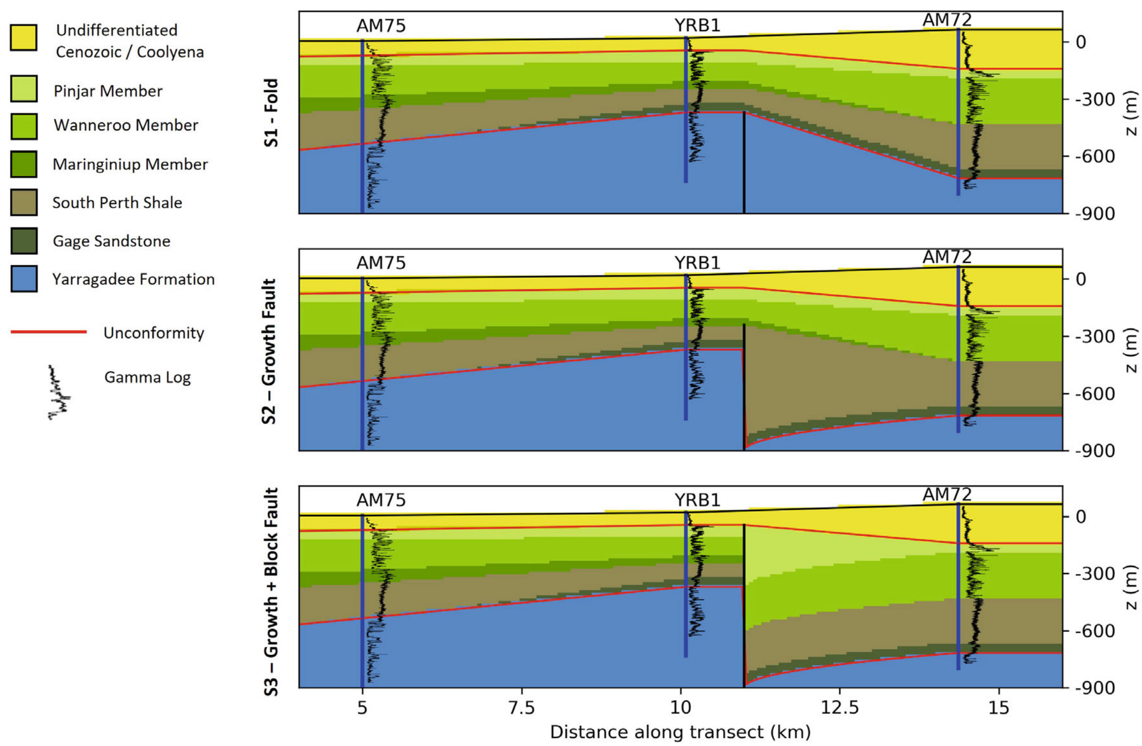

Figure 3. Three plausible structural models based on different interpretations of fault timing. Fault extent (black line), unconformities (red lines) and wells (blue lines) are shown. Gamma logs are presented for each bore. Model S1 represents a deep inactive fault in the Yarragadee but folding with all layers above. Model S2 assumes faulting occurred during deposition of the South Perth Shale resulting in growth in that formation, and then ceased. Model S3 represents deposition concurrently with faulting throughout the Early Cretaceous leaving thicker layers and block faulting on the hanging wall.

were developed for the Joondalup Fault transect, each varying in the assumption of the duration of faulting which consequently determines the offset of stratigraphy adjacent to the fault (Figure 3). Structural model S1 presents a "layer cake" interpolation and represents drape folding over a potentially deeper Joondalup Fault or could indeed represent a folded scenario. S2 assumes major faulting during deposition of the South Perth Shale, resulting in the offset and thickening of the Shale at AM72. However, it is presumed that major slip ceases at this stage so that Members of the Leederville Formation remain laterally continuous. S3 assumes continuous deposition and slip until the Aptian unconformity, resulting in a breach in the aquitard and cross-connection of the Leederville and Yarragadee aquifer. The 2D geological models were developed in Python using various interpolation functions to represent

Table 1
Parameters for Each Model Layer for the Base Case Flow Model

Parameter	Base Case Value
Hydrogeological layers	[Superficial, Coolyena, Pinjar, Wanneroo, Maringiniup, South Perth Shale, Gage, Yarragadee]
Horizontal conductivity (m/d)	[100, 0.001, 1, 6, 1, 0.001, 1.5, 1.5]
Vertical conductivity (m/d)	[1, 0.00001, 0.01, 0.06, 0.01, 0.00001, 0.015, 0.015]
Specific storage (−)	[0.0001, 0.00001, 0.0001, 0.0001, 0.0001, 0.00001, 0.0001, 0.0001]

Note: Stochastic simulations for variable layer conductivity use these conductivity values as the mean.

alternative geological interpretations. The model was constructed using a regular grid of 300 columns along 20 km and 150 layers covering a depth of 2000 m.

Base Model for Flow and Transport Model

Transient flow models were created and run for each of the three transects using FloPy and MODFLOW 6 (Langevin et al. 2017). These three models serve as the base case in that they consider only the arrangement of stratigraphic units such that the fault is only represented as juxtaposed layers without any fault zone permeability modification.

Parameters for the base models are shown in Table 1. Constant head boundaries were assigned along the west and east boundary and varied linearly with depth to replicate actual head conditions based on observation bores (see Data S1 for more details). Horizontal hydraulic conductivities for each of the eight hydrogeological layers were assigned based on the values used in the PRAMS model, and vertical conductivities were assumed to be two orders of magnitude lower than horizontal conductivity. Specific storage was based on the existing PRAMS model assumed at 10^{-4} for conductive units and 10^{-5} for shales.

A conservative tracer was injected into YRB1 to show the fate of reinjected water which replicates the actual scenario at the site. YRB1 is currently used as a recharge bore for high-quality treated wastewater. The tracer was injected over the screen interval (−371 m RL to −725 m RL) at a flow rate of 140 L/s and a nominal concentration of 100 kg/m^3 for 40 years. Longitudinal dispersivity was assumed at 1 m and transverse at 0.1 m (Gelhar et al. 1992). A uniform bulk porosity of 0.25 was adopted for simplicity given that sequences typically comprise heterogeneous layers of varying permeability and porosity.

Stochastic Simulations

Our aim was to compare the influence of structural uncertainty with uncertainty in hydraulic properties, including geological layer hydraulic properties and fault zone hydraulic properties. Therefore, we sequentially modified hydraulic conductivity for (1) geological layers; (2) fault damage zone; (3) fault core; and (4) combined layer and fault zone properties; and compared these results to the base case scenario for each structural model S1, S2, and S3. Hydraulic properties were randomly sampled for 100 realizations for each of the three categories (layer, fault damage zone, fault core). For each category sampled, the remaining categories were fixed to the base case values, resulting in 300 samples. Then, a combined scenario was conducted where all categories were sampled simultaneously 100 times. Therefore, there were a total of 400 sample sets/simulations performed. Sampling methodology is described below and visually summarized in Figure 4.

Conductivity in the principal direction for the eight geological layers was sampled from a log-normal distribution, which is typical practice in petroleum and groundwater hydrologic modeling (Nwaiwu 2009). Mean conductivities (K_{μ}) were drawn from the PRAMS model (Siade et al. 2017). The sampling range (−3o’ to +3o’)

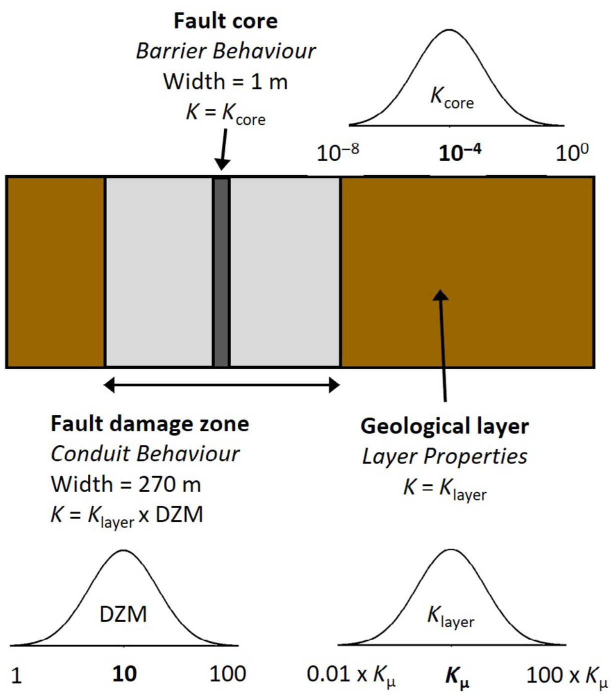

Figure 4. Conceptual fault model converted to numerical model. There are three zones whereby conductivity has been stochastically modified. The fault core exhibits barrier behavior, and its conductivity (K_{core}) is sampled from a log normal distribution with a mean of −4. The fault damage zone introduces conduit behavior by increasing conductivity via a damage zone multiplier (DZM). The DZM is sampled from a log normal distribution with a mean of 10. Lastly, the geological layer conductivity (K_{layer}) is sampled from a log normal distribution with the mean for each layer taken from the Perth Regional Aquifer Model.

was assumed two orders of magnitude below the mean and two orders of magnitude above the mean. Vertical conductivity was assumed at 100 times less than horizontal (Freeze and Cherry 1979). The fault damage zone was modeled by multiplying horizontal and vertical conductivity within an assumed damage zone by a damage zone multiplier (DZM). The damage zone was assumed to be 270 m wide, which is considered as a mean width given a maximum fault displacement of 380 m (Childs et al. 2009). The DZM was sampled from a log normal distribution with a mean of 10 and sampling range of 1 to 100. A low-permeable fault core was modeled using MODFLOW's HFB package which effectively diminishes conductance between cell faces on either side of the fault and is more efficient than using a discrete column of low conductivity. Fault core parameters used for the HFB, namely core width and conductivity, are based on published ranges using a maximum fault displacement of 380 m (Childs et al. 2009; Bense et al. 2013). A fault core width of 1 m was adopted, and the conductivity (K_{core}) sampled from a log normal distribution with a mean of 10^{-4} m/d and sampling range of 10^{-8} to 1 m/d.

Further justification of fault parameters and parameter histograms adopted for each set of 100 realizations are presented in Data S1, along with the Jupyter Notebooks used to set up the geological, flow, and transport models.

Results and Discussion

Base Case: Effect of Structure on Groundwater Flow

Head and concentration results after 40 years of injection using base case parameters without any fault zone conductivity modification are presented (Figure 5). Results are presented for each of the three structural models, S1, S2, and S3, with the injection zone defined as values greater than 5% of the injected solute concentration (5 mg/L).

Head distribution at the end of the injection period was similar for S1 and S2 (Figure 5a and 5b), but S3 (Figure 5c) shows diffusion of head through the breach in the aquitard. Similarly, solute is confined to the Yarragadee Aquifer in S1 and S2 (Figure 5a and 5b) but migrates into the upper Leederville aquifer in S3 (Figure 5c) highlighting the cross-connection of the Yarragadee Aquifer (west) to the Leederville Aquifer (east). These results indicate the importance of identifying structural scenarios where aquitards may be breached due to stratigraphy offsets at faults, which potentially results in mixing of aquifer waters.

Monte Carlo Simulations: Relative Influence of Layer Conductivity and Fault Zone Properties

Transport

Concentration results for the base case and set of 100 realizations for each structural model and conductivity modification scenario were stacked and presented as injection zone probability contours (Figure 6). The injection zones were delineated as being the extent where the concentration is above 5% of the injected solute and plotted for 90%, 50%, and 10% probabilities. Closely spaced probability contours indicate little variance in model predictions and therefore relative insensitivity to conductivity modification.

Despite dramatic changes in hydrogeological properties, groundwater movement is still clearly impacted mostly by structure, with S3 exhibiting very different solute transport (third column of Figure 6) compared to S1 and S2 (first and second column of Figure 6). S3 presents a scenario where the Leederville and Yarragadee aquifers are juxtaposed, causing hydraulic connection of two different highly conductive geological layers. Furthermore, as faulting is assumed to be more recent in S3, the fault zone propagates through the aquitard and closer to the surface. Vertical migration of injection water is therefore enhanced when high conductivity in the damage zone is introduced, with significant spreading into the highly conductive uppermost Superficial aquifer being observable in S3 (Figure 6biii). Varying layer properties introduced variability in the injection zone, but primarily for S3 (Figure 6diii). Barrier permeability seemed to affect transport relatively little, with some slight containment of the plume with barriers of very low conductivity (Figure 6ciii). Interestingly, many groundwater flow modeling studies only explicitly

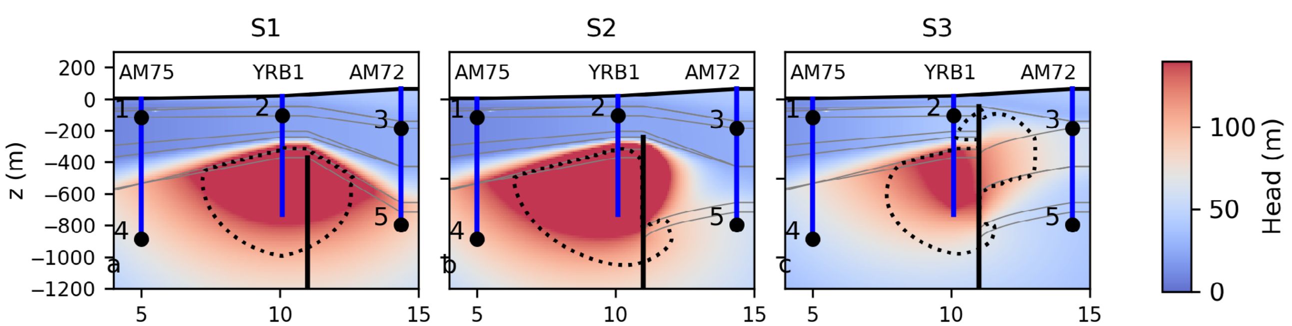

Figure 5. Head and transport results for base case scenario at the end of 40 years of injection. Final heads in meters are plotted in color as indicated in the color bar on the right. The extent of the injection zone (dotted black line) is delimited by a solute concentration above 5%. Observation points (OBS1 to OBS5) are also shown on existing bores on transect. The assumed fault extent is shown (thick black line) along with geological layer boundaries (light gray).

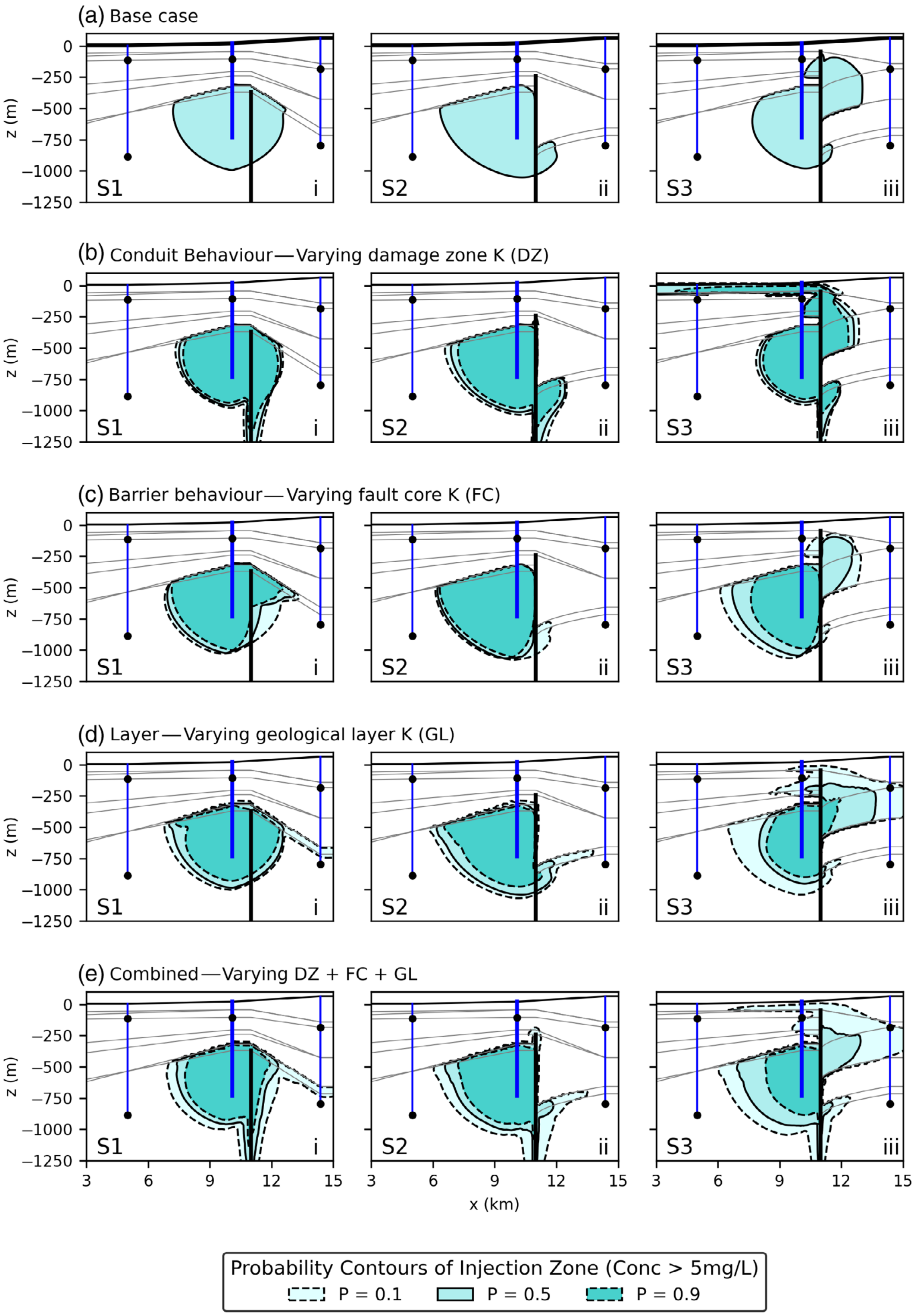

Figure 6. Probability contours of the injection zone after 40 years for varying structural models (S1, S2, and S3) and varying conductivity modification scenarios. The extent of the injection zone (dotted black line) is delimited by a solute concentration above 5%. Dark blue represents a probability of 90%, medium blue 50%, and light blue 10%. The further apart the contours, the more sensitive transport is to that scenario.

consider the barrier aspect of faults in their models (Sproule et al. 2021; Casillas-Trasvina et al. 2022), which we see here shows the lesser impact on transport than juxtaposition and conduit behavior.

Aquifer Heads

Observation points were placed in the Leederville Aquifer (OBS1, OBS2, and OBS3) and Yarragadee Aquifer (OBS4 and OBS5) to monitor the relative difference in heads over time. Their location is shown in Figure 5. Head observation probabilities of 90%, 50%, and 10% for the 40-year injection period are plotted for OBS3, OBS4, and OBS5 in Figure 7 (OBS1 and OBS2 are plotted in Data S1).

The most striking, yet unsurprising, observation is that deep Yarragadee bore heads (OBS4 and OBS5) are profoundly affected by layer conductivity (Figure 7cii and iii) given their direct hydraulic connection with the injection bore. These graphs show overlapping of head predictions between structural models indicating that head observations in these bores alone cannot assist in reducing structural uncertainty. The overlapping of head responses between structural models (Figure 7dii and iii) highlights the enormous potential for parameter bias and subsequent forward propagation of error, particularly for transport applications, if inverse modeling was applied to an incorrect structural model. Barrier behavior has a significant impact on heads in the deep aquifer where injection takes place (Figure 7bii and iii). On the other hand, conduit behavior does not greatly influence heads in observation bores (Figure 7a).

Relative Influence of Structure, Layer, and Fault Zone Conductivity Modification

The most important result from this study is that the structural model, which is a result of different interpretations on fault timing, is the most important factor affecting groundwater flow. Following structure, solute transport is controlled mostly by conduit behavior (Figure 6biii)

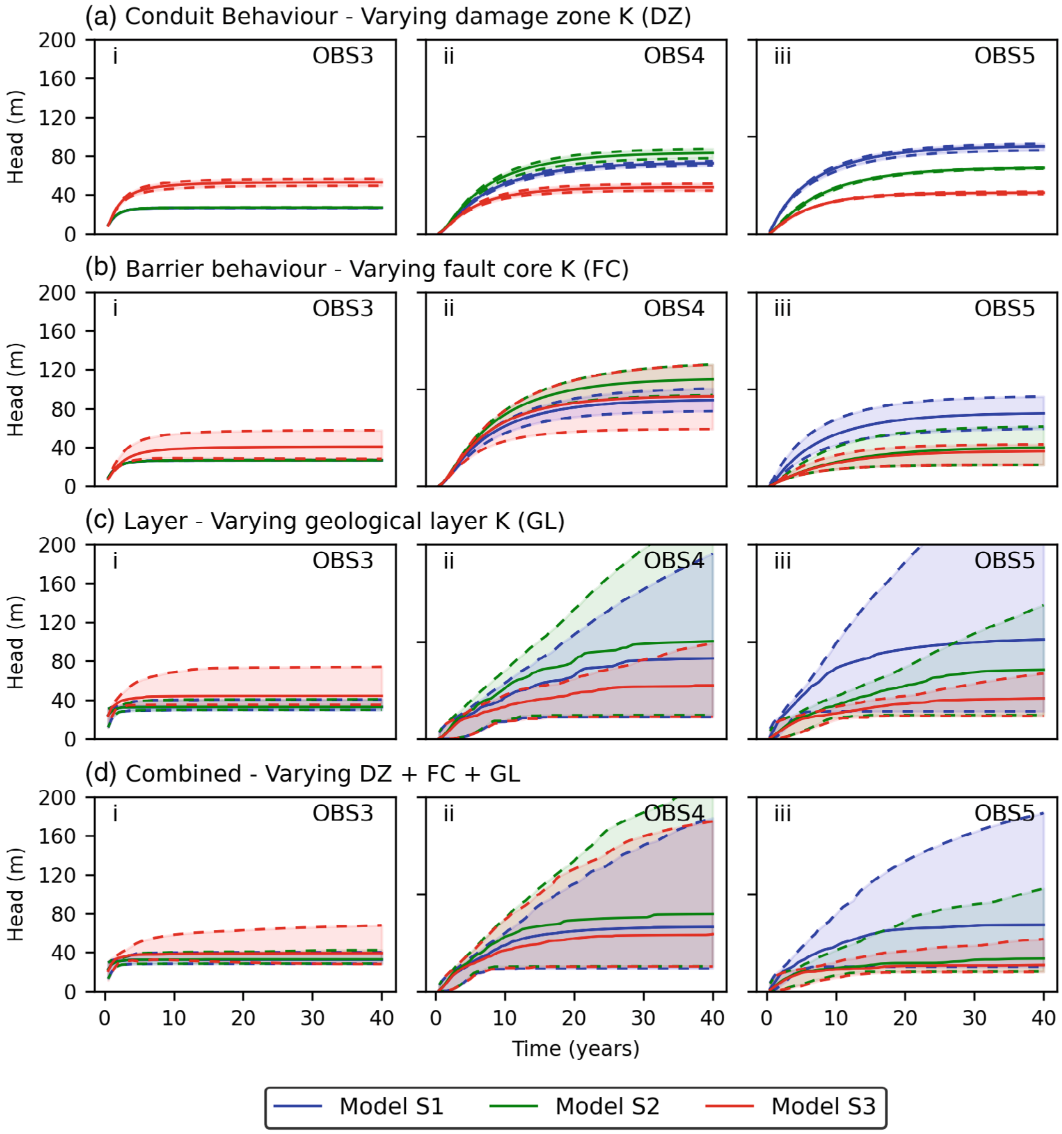

Figure 7. Predicted head for structural models S1 (blue), S2 (green), and S3 (red) over 40 years of injection for OBS3 (i), OBS4 (ii), and OBS5 (iii). Each row represents a different conductivity modification scenario (a to d). Dashed lines represent a probability of 10% and 90%, with the solid line representing the median (50% probability). Colored fill between the dashed lines therefore covers the head response in 80% of the simulations. Head is affected predominantly by layer conductivity (c and d). Due to overlapping possible head responses in c and d, head observations would not be sufficient to infer the correct structural model.

followed by layer conductivity (Figure 6diii). On the other hand, heads appear to be influenced mostly by layer conductivity (Figure 7c) followed by barrier behavior (Figure 7b). Variations in solute migration in S1 and S2 are minimal despite large variations in layer and fault zone conductivities, given that the injectant is contained beneath a sealed aquitard.

Conclusions

This study examines the effect of fault timing and stratigraphic interpretation on groundwater flow. Three different plausible stratigraphic interpretations were applied at a study site where adjacent bores showed offset and relative thickening of major units. Each interpretation assumed a different temporal extent of faulting, rather than assuming block faulting through all layers to the surface, an approach often adopted in groundwater studies. Assuming uniform offsets of layers essentially presumes all faulting occurs at the very end of a sequence of deposition, which is typically not the case. Flow modeling was undertaken on each of the three transects and included the injection of a conservative tracer over 40 years to examine predicted heads and flow pathways.

Very different pressure and transport responses were observed between the different structural models, particularly in the model incorporating the most recent faulting. In this scenario, a vertically connected pathway was introduced via juxtaposition of highly conductive layers, which was also amplified by a conductive damage zone. This scenario shows injectant traveling vertically from a deep confined aquifer through a thick aquitard and then laterally along a conductive shallow aquifer. The vertical pressure and concentration profile is significantly different between structural models, suggesting that, where faults are suspected, vertical monitoring of heads and hydrochemistry is critical in discriminating between structural models. Additionally, injected solute should be monitored in aquifers directly above injection given that breakthrough may occur quickly if nearby faults exhibit conduit behavior and extend close to surface.

Geological layer and fault zone parameters were stochastically modified to further examine the effect of these factors on flow relative to structure itself. A large potential range in layer conductivities can result in an overlapping range in head response between structural models, highlighting the enormous potential for parameter bias when using reasonable hydraulic conductivities to fit head observations for an incorrect structural model. Interestingly, this research also highlights how barrier behavior at faults affects heads but not transport, and conversely conduit behavior at faults greatly affects transport but not heads.

This paper illustrates the value of detailed consideration of realistic fault architecture based on basin history and sequence stratigraphy methods. Without sufficient evidence, faults should not be assumed to propagate to land surface, nor have uniform displacement. Appropriate allocation of resources toward additional data is needed to understand structural architecture. The collection of traditional seismic data, considered indispensable in the petroleum industry, is generally infeasible for hydrogeological investigations due to expense and limitations in built-up areas. Therefore, detailed downhole geophysical and palynological data must be used instead, preferably alongside passive seismic or other 2D geophysical methods where possible. Where additional data collection is prohibitive, multiple structural models should be used to adequately address predictive uncertainty. Careful geological modeling of faults which considers sequence stratigraphy and basin tectonics is also needed to address the importance of fault timing. Layer cake interpolation with simple block faulting between sparse bore logs may inadvertently ignore critical vertical flow pathways.

Acknowledgments

This study was financially supported by the Australian Research Council, Department of Water and Environmental Regulation of Western Australia, Water Corporation of Western Australia and Rio Tinto Iron Ore through Grant Number LP180101153. The authors thank Clive Hampton and Jon-Philippe Pigois for their reviews, as well as the two anonymous reviewers and Charles Andrews, the Executive Editor. Open access publishing facilitated by The University of Western Australia, as part of the Wiley - The University of Western Australia agreement via the Council of Australian University Librarians.

Authors' Note

The authors do not have any conflicts of interest or financial disclosures to report.

Data Availability Statement

The data that support the findings of this study are available from Water Corporation of Western Australia. Restrictions apply to the availability of these data, which were used under license for this study. Data are available from the author(s) with the permission of Water Corporation of Western Australia.

Supporting Information

Additional supporting information may be found online in the Supporting Information section at the end of the article. Supporting Information is generally *not* peer reviewed.

Data S1. Selecting representative fault parameters for the Joondalup Fault.

References

Ainsworth, R.B. 2006. Sequence stratigraphic-based analysis of reservoir connectivity: Influence of sealing faults – A case study from a marginal marine depositional setting. *Petroleum Geoscience* 12, no. 2: 127–141.

Ainsworth, R.B. 2005. Sequence stratigraphic-based analysis of reservoir connectivity: Influence of depositional architecture – A case study from a marginal marine depositional setting. *Petroleum Geoscience* 11: 257–276.
Allan, U.S. 1989. Model for hydrocarbon migration and entrapment within faulted structures. *American Association of Petroleum Geologists Bulletin* 73, no. 7: 803–811.
Bardot, K., M. Lesueur, A.J. Siade, and J.L. McCallum. 2022. Revisiting MODFLOW's capability to model flow through sedimentary structures. *Groundwater* 61, no. 5: 663–673.
Bense, V.F., T. Gleeson, S.E. Loveless, O. Bour, and J. Scibek. 2013. Fault zone hydrogeology. *Earth-Science Reviews* 127: 171–192.
Bense, V.F., and M. Person. 2006. Faults as conduit-barrier systems to fluid flow in siliciclastic sedimentary aquifers. *Water Resources* 42, no. 5: 1–18.
Bredehoeft, J. 2005. The conceptualization model problem—Surprise. *Hydrogeology Journal* 13: 37–46.
Caine, J.S., J.P. Evans, and C.B. Forster. 1996. Fault zone architecture and permeability structure. *Geology* 24, no. 11: 1025–1028.
Casillas-Trasvina, A., B. Rogiers, K. Beerten, L. Wouters, and K. Walraevens. 2022. Exploring the hydrological effects of normal faults at the boundary of the Roer Valley Graben in Belgium using a catchment-scale groundwater flow model. *Hydrogeology Journal* 30, no. 1: 133–149.
Childs, C., T. Manzocchi, J.J. Walsh, C.G. Bonson, A. Nicol, and M.P.J. Schöpfer. 2009. A geometric model of fault zone and fault rock thickness variations. *Journal of Structural Geology* 31, no. 2: 117–127.
Crostella, A., and J. Backhouse. 2000. Geology and petroleum exploration of the Central and Southern Perth Basin, Geological Survey of Western Australia, Report 57.
Davidson, W. A. 1995. Hydrogeology and groundwater resources of the Perth Region, Western Australia. Geological Survey of Western Australia, Bulletin 142.
De Silva, J., P. Wallace-Bell, C. Yesertener, and S. Ryan. 2013. Perth Regional Aquifer Modelling System (PRAMS) v3.5 – Conceptual Model. Department of Water and Environmental Regulation, Western Australia, HG20.
Enemark, T., L.J.M. Peeters, D. Mallants, and O. Batelaan. 2019. Hydrogeological conceptual model building and testing: A review. *Journal of Hydrology* 569: 310–329.
Freeze, A.R., and J.A. Cherry. 1979. *Groundwater*. Englewood Cliffs: Prentice-Hall.
Gelhar, L., C. Welt, and K. Rehfeldt. 1992. A critical review of data on field-scale dispersion in aquifers. *Water Resources Research* 28, no. 7: 1955–1974.
Grose, L., L. Ailleres, G. Laurent, and M. Jessell. 2021. LoopStructural 1.0: Time-aware geological modelling. *Geoscientific Model Development* 14, no. 6: 3915–3937.
Hadley, D.R., D.B. Abrams, and G.S. Roadcap. 2020. Modeling a large-scale historic aquifer test: Insight into the hydrogeology of a regional fault zone. *Groundwater* 58, no. 3: 453–463.
Hojberg, A., and J.C. Refsgaard. 2005. Model uncertainty – Parameter uncertainty versus conceptual models. *Water Science and Technology* 52, no. 6: 177–186.
HydroAlgorithmics. 2020. *AlgoMesh 2 User Guide*. Australia: HydroAlgorithmics Pty Ltd.
Knipe, R.J. 1997. Juxtaposition and seal diagrams to help analyze fault seals in hydrocarbon reservoirs. *AAPG Bulletin* 81, no. 2: 187–195.
Langevin, C.D., J.D. Hughes, E.R. Banta, R.G. Niswonger, S. Panday, and A.M. Provost. 2017. Documentation for the MODFLOW 6 Groundwater Flow Model: U.S. Geological Survey Techniques and Methods 6-A55.
Leray, S., J.R. de Dreuzy, O. Bour, T. Labasque, and L. Aquilina. 2012. Contribution of age data to the characterization of complex aquifers. *Journal of Hydrology* 464–465: 54–68.
Leyland, L. 2012. Reinterpretation of the Hydrogeology of the Leederville Aquifer Gnangara Groundwater System. Department of Water and Environment of Western Australia, HG59.
Li, X., and F.T.C. Tsai. 2009. Bayesian model averaging for groundwater head prediction and uncertainty analysis using multimodel and multimethod. *Water Resources Research* 45, no. 9: 1–14.
Manzocchi, T., C. Childs, and J.J. Walsh. 2010. Faults and fault properties in hydrocarbon flow models. *Geofluids* 10: 94–113.
Manzocchi, T., J.J. Walsh, P. Nell, and G. Yielding. 1999. Fault transmissibility multipliers for flow simulation models. *Petroleum Geoscience* 5: 53–63.
Marshall, S., P. Cook, A. Miller, C. Simmons, and S. Dogramaci. 2019. The effect of undetected barriers on groundwater drawdown and recovery. *Groundwater* 57, no. 5: 718–726.
McCallum, J.L., S.L. Noorduijn, and C.T. Simmons. 2021. Including vertical fault structures in layered groundwater flow models. *Groundwater* 59, no. 6: 799–807.
Michael, H.A., H. Li, A. Boucher, T. Sun, J. Caers, and S.M. Gorelick. 2010. Combining geologic-process models and geostatistics for conditional simulation of 3-D subsurface heterogeneity. *Water Resources Research* 46, no. 5: 1–20.
Mory, A.J., and R.P. Iasky. 1996. Stratigraphy and structure of the onshore northern Perth Basin. Conference Paper: The Sedimentary Basins of Western Australia. Perth, Western Australia.
Nishikawa, T., A.J. Siade, E.G. Reichard, D.J. Ponti, A.G. Canales, and T.A. Johnson. 2009. Stratigraphic controls on seawater intrusion and implications for groundwater management, Dominguez Gap Area of Los Angeles, California, USA. *Hydrogeology Journal* 17, no. 7: 1699–1725.
Nwaiwu, C. 2009. Statistical distributions of hydraulic conductivity from reliability analysis data. *Geotechnical and Geological Engineering* 27, no. 1: 169–179.
Olierook, H.K.H., N.E. Timms, R.E. Merle, F. Jourdan, and P.G. Wilkes. 2015. Paleodrainage and fault development in the southern Perth Basin, Western Australia during and after the breakup of Gondwana from 3D modelling of the Bunbury Basalt. *Australian Journal of Earth Sciences* 62, no. 3: 289–305.
Ortiz, J.P., M.A. Person, P.S. Mozley, J.P. Evans, and S.L. Bilek. 2019. The role of fault-zone architectural elements on pore pressure propagation and induced seismicity. *Groundwater* 57, no. 3: 465–478.
Pham, H.V., and F.T.C. Tsai. 2016. Optimal observation network design for conceptual model discrimination and uncertainty reduction. *Journal of the American Water Resources Association* 52: 1245–1264.
Poulet, T., M. Lesueur, and U. Kelka. 2021. Dynamic modelling of overprinted low-permeability fault cores and surrounding damage zones as lower dimensional interfaces for multiphysics simulations. *Computers and Geosciences* 150: 104719.
Refsgaard, J.C., S. Christensen, T. Sonnenborg, D. Seifert, A.L. Højberg, and L. Troldborg. 2012. Review of strategies for handling geological uncertainty in groundwater flow and transport modeling. *Advances in Water Resources* 36: 36–50.
Refsgaard, J.C., J.P. van der Sluijs, J. Brown, and P. van der Keur. 2006. A framework for dealing with uncertainty due to model structure error. *Advances in Water Resources* 29, no. 11: 1586–1597.
Rojas, R., L. Feyen, and A. Dassargues. 2008. Conceptual model uncertainty in groundwater modeling: Combining generalized likelihood uncertainty estimation and Bayesian Model averaging. *Water Resources Research* 44, no. 12: 1–16.
Rongier, G., P. Collon, and P. Renard. 2017. Stochastic simulation of channelized sedimentary bodies using a

constrained L-system. *Computers & Geosciences* 105: 158–168.
Scharling, P.B., E.S. Rasmussen, and K. Hinsby. 2009. Three-dimensional regional-scale hydrostratigraphic modeling based on sequence stratigraphic methods: A case study of the Miocene succession in Denmark. *Hydrogeology Journal* 17: 1913–1933.
Schlische, R.W., and M.H. Anders. 1996. Stratigraphic effects and tectonic implications of the growth of normal faults and extensional basins. In *Reconstructing the History of Basin and Range Extension Using Sedimentology and Stratigraphy*, ed. Kathi K. Beratan. McLean, Virginia, USA: Geological Society of America.
Seifert, D., T.O. Sonnenborg, J.C. Refsgaard, A.L. Højberg, and L. Troldborg. 2012. Assessment of hydrological model predictive ability given multiple conceptual geological models. *Water Resources Research* 48, no. 6: 1–16.
Siade, A.J., J. Hall, and R.N. Karelse. 2017. A practical, robust methodology for acquiring new observation data using computationally expensive groundwater models. *Water Resources Research* 53, no. 11: 9860–9882.
Song, T., and P.A. Cawood. 2000. Structural styles in the Perth Basin associated with the Mesozoic break-up of greater India and Australia. *Tectonophysics* 317, no. 1–2: 55–72.
Song, T., and P.A. Cawood. 1999. Multistage deformation of linked fault systems in extensional regions: An example from the northern Perth Basin, Western Australia. *Australian Journal of Earth Sciences* 46, no. 6: 897–903.
Sproule, T.G., G.A. Spinelli, J.L. Wilson, M.D. Fort, P.S. Mozley, and J. Ciarico. 2021. The effects of fault-zone cementation on groundwater flow at the field scale. *Groundwater* 59, no. 3: 396–409.
Thomas, CM. 2014. The tectonic framework of the Perth Basin: current understanding: Geological Survey of Western Australia, Record 2014/14.
Troldborg, L., J.C. Refsgaard, K.H. Jensen, and P. Engesgaard. 2007. The importance of alternative conceptual models for simulation of concentrations in a multi-aquifer system. *Hydrogeology Journal* 15, no. 5: 843–860.
White, J.T., R.J. Hunt, M.N. Fienen, and J. Doherty. 2020. Approaches to Highly Parameterized Inversion: PEST++ Version 5, a Software Suite for Parameter Estimation, Uncertainty Analysis, Management Optimization and Sensitivity Analysis. U. S. Geological Survey Techniques and Methods 7-C26.
Yielding, G., B. Freeman, and D.T. Needham. 1997. Quantitative fault seal prediction. *AAPG Bulletin* 81, no. 6: 897–917.
Zhou, Y., and W. Li. 2011. A review of regional groundwater flow modeling. *Geoscience Frontiers* 2, no. 2: 205–214.